

Research Article

Biochemical detection of fatal hypothermia and hyperthermia in affected rat hypothalamus tissues by Fourier transform infrared spectroscopy

Hancheng Lin^{1,2,*}, Kaifei Deng^{1,*}, Ji Zhang¹, Lei Wang¹, Zhong Zhang¹, Yiwen Luo¹, Qiran Sun¹, Zhengdong Li¹, Yijiu Chen¹, Zhenyuan Wang² and  Ping Huang¹

¹Shanghai Key Laboratory of Forensic Medicine, Shanghai Forensic Service Platform, Academy of Forensic Science, Shanghai 200063, China; ²Department of Forensic Pathology, Xi'an Jiaotong University, Xi'an 710061, China

Correspondence: Ping Huang (huangp@ssfjd.cn) or Zhenyuan Wang (wzy218@mail.xjtu.edu.cn)



It is difficult to determinate the cause of death from exposure to fatal hypothermia and hyperthermia in forensic casework. Here, we present a state-of-the-art study that employs Fourier-transform infrared (FTIR) spectroscopy to investigate the hypothalamus tissues of fatal hypothermic, fatal hyperthermic and normothermic rats to determine forensically significant biomarkers related to fatal hypothermia and hyperthermia. Our results revealed that the spectral variations in the lipid, protein, carbohydrate and nucleic acid components are highly different for hypothalamuses after exposure to fatal hypothermic, fatal hyperthermic and normothermic conditions. In comparison with the normothermia group, the fatal hypothermia and hyperthermia groups contained higher total lipid amounts but were lower in unsaturated lipids. Additionally, their cell membranes were found to have less motional freedom. Among these three groups, the fatal hyperthermia group contained the lowest total proteins and carbohydrates and the highest aggregated and dysfunctional proteins, while the fatal hypothermia group contained the highest level of nucleic acids. In conclusion, this study demonstrates that FTIR spectroscopy has the potential to become a reliable method for the biochemical characterization of fatal hypothermia and hyperthermia hypothalamus tissues, and this could be used as a postmortem diagnostic feature in fatal hypothermia and hyperthermia deaths.

Introduction

Thermoregulation, as one important aspect of human homeostasis, keeps the body temperature of the organism within certain boundaries [1]. The prolonged exposure to extreme ambient temperature (fatal hypothermia and hyperthermia) can induce the breakdown of the internal thermoregulatory control and finally, especially for the very young and the elderly, lead to death [2,3]. The identification of hypothermia and hyperthermia as the cause of death is usually difficult in forensic casework because of unspecific, irregular or even negative macroscopic and microscopic findings [2–7]. In order to better understand the pathophysiology of fatal hypothermia and hyperthermia, numerous postmortem biochemical investigations of biochemical markers such as electrolytes, hormones, blood proteins, enzymes and neurotransmitters, in the blood and other biological fluids, have been performed in the last several decades [2–4,8–16]. However, the practical applications of these biochemical investigation results need to be confirmed through targeted studies on larger sample groups of hypothermia/hyperthermia-related deaths.

The hypothalamus is the main seat of thermoregulation, and its metabolic and functional activity changes as the core temperature of the body changes [17]. Therefore, it is reasonable to expect that a good knowledge of the biochemical hypothalamus response to fatal hypothermic/hyperthermic stress would be

* These authors contributed equally to this work.

Received: 16 September 2018

Revised: 16 February 2019

Accepted: 27 February 2019

Accepted Manuscript Online:
01 March 2019

Version of Record published:
15 March 2019

beneficial for the determination of fatal hypothermia/hyperthermia. However, only a few of the published studies on hypothalamus tissue discuss the changes of specific immunohistochemistry-specific markers, like catecholamines [18] and chromogranin A [19], in response to fatal hypothermia/hyperthermia. The overall biochemical response of the hypothalamus is still unclear. It would be highly advantageous to implement a simple and rapid method for the acquisition of total biomolecular composition and the variations, to be able to analyze hypothalamus tissue for forensic cases.

Fourier-transform infrared (FTIR) spectroscopy is a qualitative and quantitative analytical technique that is commonly used in the fields of biomedical science, materials science and medicine [20–22]. The principle of infrared spectroscopy is to utilize an infrared source-induced molecular motion to generate a signature fingerprint of chemical components in the form of spectrum [23]. The increased improvement in both instrumentation (such as surface enhanced infrared spectroscopy, quantum cascade laser infrared spectroscopy and atomic force microscopy infrared spectroscopy) [24–26] and chemometric methods (such as artificial neural network, support vector machine, random forest algorithm and linear discriminant analysis) [27] has seen infrared spectroscopy become a powerful technique for analyzing biological samples, like cells, tissues and biological fluids. The most commonly used infrared region for biological applications is the mid-IR region ($4000\text{--}400\text{ cm}^{-1}$), which includes the $3100\text{--}2800\text{ cm}^{-1}$ region, mainly representative of lipids, and the so-called fingerprint region ($1800\text{--}900\text{ cm}^{-1}$), mainly representative of amide I/II, lipids, carbohydrates and nucleic acids [28]. The greatest benefit of FTIR technique lies in its highly sensitive acquisition of the whole ‘-omics’ of a biological sample, which enables the detection of molecular changes that may reflect the onset and progression of a disease, thus enabling disease diagnosis and monitoring [29]. Up to now, this technique has been widely used in the medical field for cancer diagnoses, such as skin [30], breast [31,32], cervical [33], colon [34] and kidney tumors [35], detections of antibiotics’ resistant *Escherichia coli* bacteria [36], human papillomavirus [37] and malaria infected red blood cells [38], and monitoring of tendinopathy [39] and chronic venous leg ulcer exudates [40].

The potential of FTIR techniques is also highlighted in the research of neurodegenerative diseases, like Alzheimer’s disease [41–44], Parkinson’s disease [45–47] and multiple sclerosis [48], since FTIR spectroscopy is sensitive to protein aggregation, which is regarded as the hallmark of neurodegenerative diseases in an emerging concept in the field of central nervous system diseases [49]. Additionally, there is abundant literature reporting the applications of FTIR spectroscopy to other neurological diseases such as, cerebral malaria [50], ischemic stroke [51–54], hemorrhagic stroke [55] and epilepsy [56,57], in human and animal models. These published studies demonstrate neurological disease-related biochemical alternations such as protein misfolding and aggregation, lipid oxidation, abnormal carbohydrate metabolism and DNA/RNA unusual expression, all monitored by FTIR spectroscopy.

Given the powerful capacity of FTIR spectroscopy for detecting specific spectral biomarkers for brain tissues with various pathological conditions, we established a state-of-the-art study that employed the FTIR technique with a combination of chemometric methods to investigate the biochemical changes of hypothalamus tissues in response to fatal hypothermia, fatal hyperthermia and normothermia in rat models. Hypothalamus not only regulates body temperature, but also controls hunger, important aspects of parenting and attachment behaviors, thirst, fatigue, sleep and circadian rhythms [58]. It’s reasonable to believe that except the temperature factor, changes of the other factors could also lead to alternations of hypothalamus functions and biochemical properties. To eliminate the effects of these factors on the biochemical properties of hypothalamus tissue, a targeted feeding programme for experimental rats was designed in this study. Ultimately, it is guaranteed that the changes of biochemical properties of hypothalamus are mainly the result of pathophysiological processes induced by extreme temperature and(or) the result of the direct physical effect of extreme temperature on the hypothalamus tissue. The aim of our study is to identify differences and similarities in the proteomic, lipidemic, genomic and metabolic components of the fatal hypothermic, fatal hyperthermic and normothermic hypothalamus tissues. The comparison of these could give new insights into the pathophysiological process of the hypothalamus in response to fatal hypothermia and hyperthermia stress. Furthermore, the specific spectrochemical markers that determined by chemometric methods may serve us to develop new method for postmortem diagnosis of fatal hypothermia and hyperthermia.

Materials and methods

Animal preparation

The study was conducted in strict accordance with the recommendations in the Guide for the Care and Use of Laboratory Animals of Xi’an Jiaotong University. The protocol was approved by the Committee on the Ethics of Animal Experiments of Xi’an Jiaotong University. Every effort was made to minimize animal suffering. Forty-seven male Sprague–Dawley rats weighing 260–300 g (provided by the Animal Centre of Xi’an Jiaotong University) were used

for the experiment. The rat models were established as described previously [59,60]. Briefly, the rats were kept for one week in stainless steel cages at $23 \pm 2^\circ\text{C}$ until physical conditions were stabilized in a 12-h light/dark environment. Food and water were supplied *ad libitum*. Then, the rats were anaesthetized with an intraperitoneal injection of pentobarbital sodium (50 mg/kg) and randomly divided into three groups. In the fatal hyperthermia group ($n=17$), the rats were exposed to an ambient temperature of 43°C in a temperature-controlled chamber with relative humidity of 60% until death (average death time, 80 min). In the fatal hypothermia group ($n=17$), the dorsal and abdominal hair of the rats were shaved and thereafter the area was immersed in ethanol (96%) for about 10 s. After ethanol exposure, the rats were placed in a cold room at 4°C until death (average death time, 120 min). In the control group ($n=13$), rats were humanely sacrificed through decapitation. When each rat was confirmed dead, its brain was removed rapidly, then snap-frozen with liquid nitrogen and stored at -80°C until the FTIR experiments. Just before the experiment, a brain sample was taken from the freezer and two adjacent 10- μm -thick coronal sections of the brain were cut with a cryo-microtome at -18°C . The details about the selection of specific brain coronal sections for infrared measurement are presented in Supplementary Figure S1. One section was melted onto a CaF_2 substrate, and then air-dried for a period of 2 min for immediate FTIR imaging analysis. The other section was mounted on a conventional glass slide and stained with hematoxylin&eosin (H&E).

FTIR spectroscopic analysis

FTIR spectroscopic images were collected using a Nicolet iN10 MX infrared microscope (Thermo Fisher Scientific, Waltham, MA, USA) equipped with a liquid nitrogen cooled 16-element mercury-cadmium-telluride linear array detector. The OMNIC Picta software 9.0 (Thermo Fisher Scientific, Waltham, MA, USA) was used for instrument control and spectral data acquisition. In this study, the spatial and spectral resolutions were set to $25 \times 25 \mu\text{m}^2$ and 4 cm^{-1} . Spectra were acquired with the co-addition of 32 scans over the range $4000\text{--}900 \text{ cm}^{-1}$. A background image was collected from a blank substrate before the collection of each sample image. FTIR spectroscopic images of samples mounted on CaF_2 slides were collected in transmission mode. In these conditions, approximately 4 min were needed to collect an infrared image containing 160 spectra and corresponding to a typical hypothalamus area of $250 \times 400 \mu\text{m}^2$. It should be mentioned that before each measurement, the specific area of hypothalamus was confirmed by a professional pathologist. A total of 47 images (an image per sample) were finally recorded. A row spectral data set containing 7520 spectra (2720 for the fatal hypothermia group, 2720 for the fatal hyperthermia group and 2080 for the normothermia group) were gathered from these 47 images and then subjected to data pre-processing.

Spectral data pre-processing and analysis

First, a 4-point baseline, passing by 3100 , 2800 , 1800 and 899 cm^{-1} , was subtracted from each spectrum. Subsequently, the spectral dataset was subjected to extended multiplicative signal correction (EMSC) [61] to normalize the spectra and remove scattering effects. Finally, the dimensionalities of the spectral dataset were reduced to the $3100\text{--}2800$ and $1800\text{--}900 \text{ cm}^{-1}$, two specific regions dominated by the spectral features of biochemical components such as lipids, proteins, carbohydrates and nucleic acids. The pre-processed spectra were then subjected to principle component analysis (PCA) and random forest (RF). PCA is a classic unsupervised multivariate algorithm that can be used to categorize the samples based on the differences between the spectra [62]. PCA offers two important outcomes: one is PC-scores, which provides a way to understand and visualize the distribution of complex spectral datasets; the other is PC-loadings, which helps us identify new meaningful spectral variables underlying the distribution. RF is a supervised classification method whose one parameter, Mean Decrease in Gini Coefficient, could reveal important distinguishing wavenumbers [63]. PCA and RF were both implemented in this study to mine specific spectral features responsible for the discrimination of fatal hypothermic, fatal hyperthermic and normothermic hypothalamus tissues.

The pre-processing of the raw spectral dataset was performed using Unscrambler 10.3X (Camosoftware, Oslo, Norway). PCA was performed using the Statistics Toolbox built into MATLAB 2014a (MathWorks Inc., Natick, MA, USA). RF analysis was conducted using the 'RandomForest' Package (version 4.6-12) implemented in R 3.4.1.

Statistical analysis

Normality of data was not guaranteed, so nonparametric methods of statistical analysis were adopted in this study. All data are presented as medians together with interquartile ranges. The statistical significance of differences between the analyzed groups was assessed by Kruskal–Wallis test. Nemenyi test was applied for multiple comparisons. A probability value of < 0.05 was considered significant. The statistical analysis was performed using the Statistics Toolbox built into MATLAB 2014a (MathWorks Inc., Natick, MA, USA).

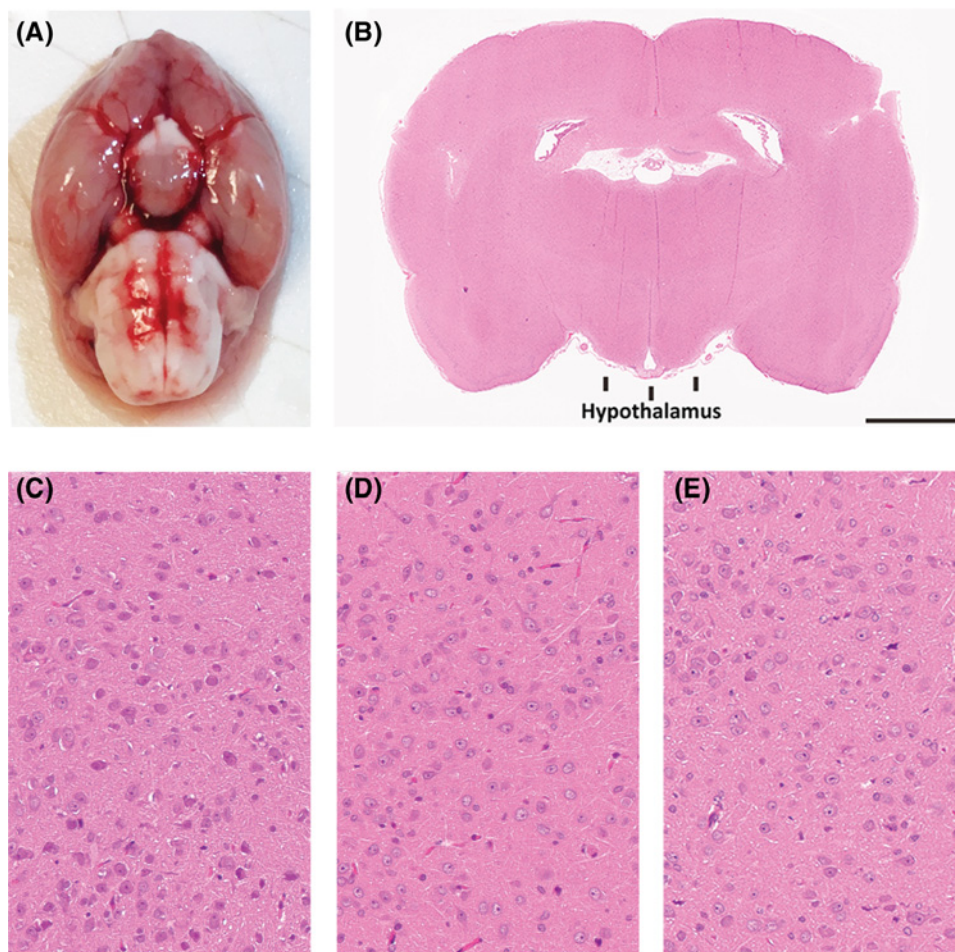


Figure 1. Histopathological results of the rat hypothalamus tissues

(A) Normothermic rat brain annotated with an oval indicating the hypothalamus position; scale bar represents 2.5 mm. (B) Whole slide scan of an H&E stained normothermic brain tissue section annotated with a square indicating the IR measurement area of hypothalamus tissue. H&E staining results of the fatal hypothermic (C), hyperthermic (D) and normothermic (E) hypothalamus tissues; Scale bar represents 50 μm .

Results and discussion

Histopathological analysis

Histopathological analysis is a conventional procedure for forensic post-mortem examination. Generally, clear histopathological findings can help the examiner determine the antemortem pathophysiological state of the tissues [64]. In this study, to examine histopathological changes, the three groups of hypothalamus tissues were stained with H&E. An edematous and congestive characteristic of the hypothalamus was generally observed in the fatal hypothermic and hyperthermic samples (Figure 1). However, these findings are regarded as nonspecific in forensic pathology because similar changes can be observed in other cases with different causes of death.

FTIR difference spectra analysis

The EMSC normalized and averaged IR spectra of the three groups of hypothalamus tissue are displayed in Figure 2A. However, these three averaged spectra seem to be very similar at first glance. Therefore, in our next step, differential spectrum analysis was applied to capture the subtle spectral alterations. Figure 2B displays the new spectra calculated from the mean absorbance spectra shown in Figure 2A. The positive and negative signals representing absorbance differences are noticed mainly in the lipid region ($3100\text{--}2800\text{ cm}^{-1}$), protein amide I and II bands ($1700\text{--}1500\text{ cm}^{-1}$) and carbohydrate and nucleic acid region ($1200\text{--}900\text{ cm}^{-1}$), indicative of the proteomic, lipidic, genomic and metabolic variations among the fatal hypothermic, fatal hyperthermic and normothermic hypothalamus tissues.

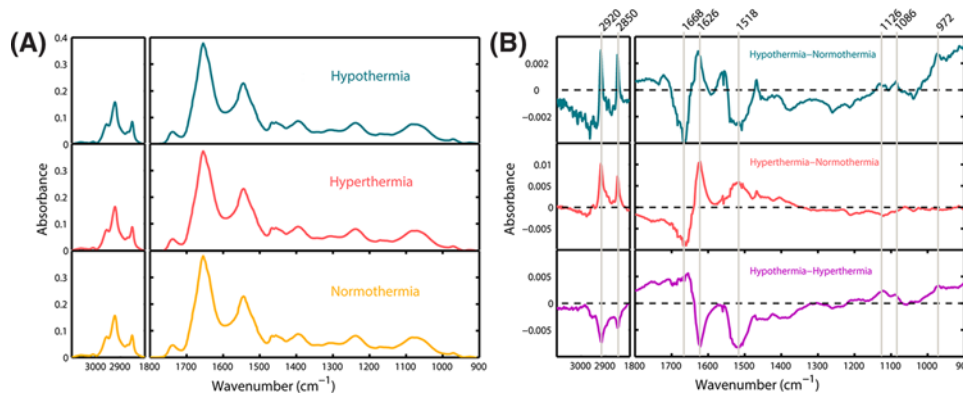


Figure 2. Results of FTIR spectral analysis

(A) EMSC normalized and averaged IR spectra of fatal hypothermic, fatal hyperthermic and normothermic hypothalamus tissues. (B) IR difference spectra (i.e. hypothermia–normothermia, hyperthermia–normothermia and hypothermia–hyperthermia).

When the averaged absorbance spectrum of the normothermia group was subtracted from the fatal hypothermia and hyperthermia groups, their resultant difference spectra show quite similar band shapes in the lipid (3100–2800 cm^{-1}) and protein amide I (1700–1600 cm^{-1}) regions. In comparison with the normothermia group, the absorbance value at around 2850 and 2920 cm^{-1} , attributed to the CH_2 symmetric and asymmetric stretching mode of the fatty acids [65], increases in both the fatal hypothermia and hyperthermia groups. The observation of the negative peak at 1668 cm^{-1} (assigned as β -turn structures) [66] and the positive peak at 1626 cm^{-1} (assigned as β -sheet structures) [65] clearly demonstrates alterations of the secondary structures of regular proteins. However, the band shapes below 1530 cm^{-1} in the resultant difference spectra are quite different. The absorbance value at around 1518 cm^{-1} , arising from tyrosine side chains [67], decreases in the case of the fatal hypothermia group but increases in the case of the fatal hyperthermia group. This finding suggests a different concentration of tyrosine-rich proteins in the fatal hypothermia and hyperthermia groups. Additionally, two positive peaks around 1086 and 972 cm^{-1} were detected for fatal hypothermia group; the 1086 cm^{-1} peak arises from symmetric PO_2^- stretching of phosphodiester groups that could be found in DNA, RNA and phospholipids [65] and 972 cm^{-1} is attributed to C-C/C-O stretching of deoxyribose-ribose vibration of DNA [68,69]. These two positive peaks taken together suggest the existence of a higher amount of nucleic acids in the fatal hypothermia group in comparison with the normothermia group. In addition, another prominent IR peak that should be highlighted is the 1126 cm^{-1} , an important spectral marker for lactate [51]. The increase and decrease for the fatal hypothermia and hyperthermia spectra respectively, in comparison with the normothermia spectrum, are indicative of different lactate concentrations in fatal hypothermic and hyperthermic hypothalamus tissues.

Principle component analysis

PCA was employed to differentiate the FTIR-based profiles of hypothalamus tissues in the fatal hypothermia, fatal hyperthermia and normothermia groups. In the first step, for each spectroscopic image, every ten spectra randomly extracted from the corresponding spectral dataset were averaged to represent one spectrum. A spectrum that had been selected once for computing a mean spectrum was not allowed to be selected again for the computation of another mean spectrum. Consequently, 272, 272 and 208 mean spectra, corresponding to the fatal hypothermia, fatal hyperthermia and normothermia groups, respectively, were calculated and then mean-centered for PCA. The PCA results, presented as scores and loadings plots for fatal hypothermia-control, fatal hyperthermia-control and fatal hypothermia-fatal hyperthermia groups are displayed in Figure 3A–C, respectively. As seen in this figure, each score's plot shows a clear binary separation. The loadings plots that identify new meaningful variables responsible for the discrimination of the groups appearing in the scores plots are also shown in Figure 3A–C. The 'M'-shape and inverted 'N'-shape observed in the 3100–2800 cm^{-1} and 1700–1600 cm^{-1} regions of the PC-loadings plot for Figure 3A,B could underline both an increase in the lipid components and an alteration in the secondary conformational structures of the proteins of fatal hypothermia and hyperthermia groups in comparison with the normothermia group. These findings are in accordance with our aforementioned results of the differential spectra analysis. Additionally, multiple positive and negative peaks observed in the 3100–2800 and 1700–900 cm^{-1} regions of the PC-loadings plot for Figure 3C indicate varying concentrations of biomolecules in the fatal hypothermia and hyperthermia groups.

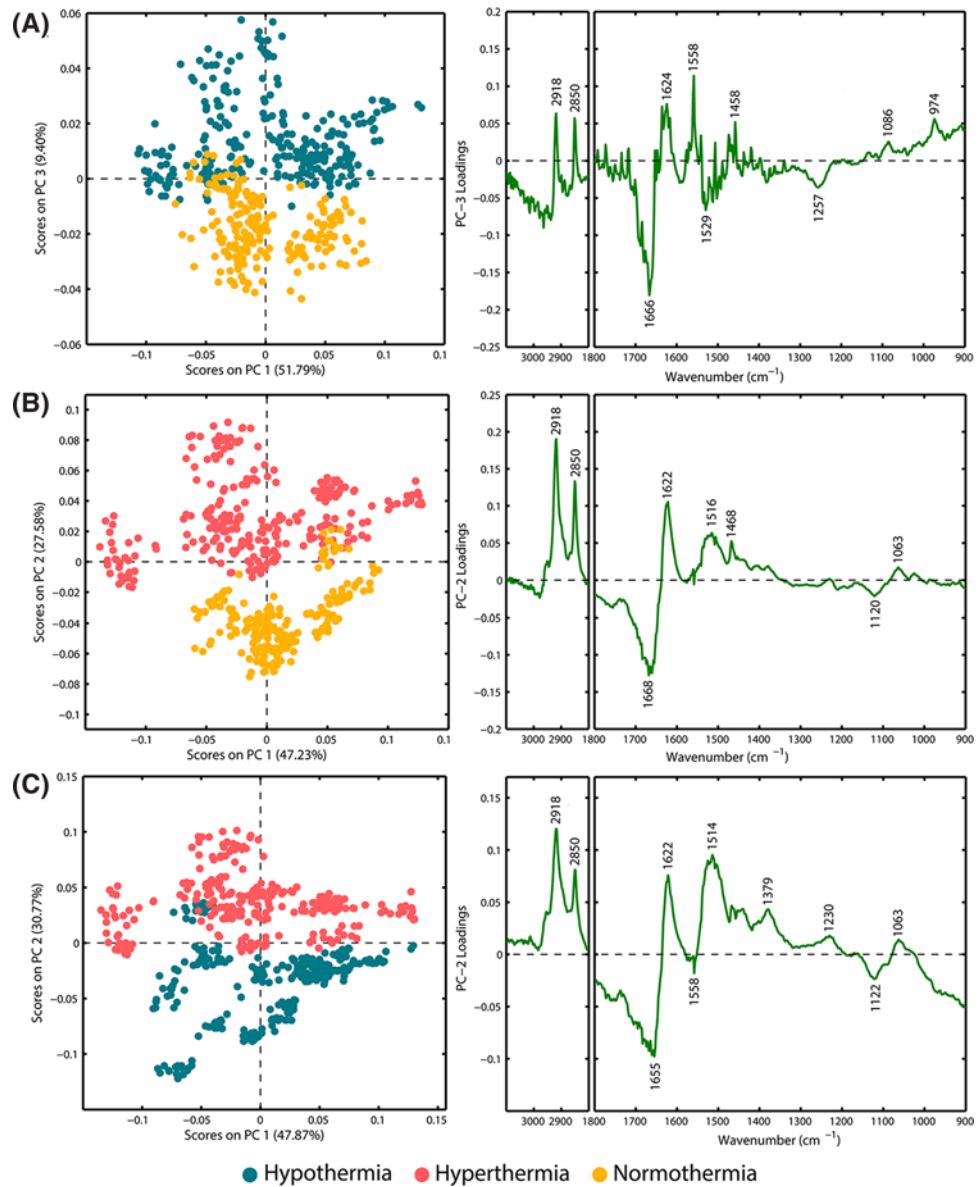


Figure 3. PCA score and loading plots

(A) PCA results for spectra from fatal hypothermia and normothermia hypothalamus tissues: scores plot (PC-1 vs. PC-3) and loading corresponding to PC-3); (B) PCA results for spectra from fatal hyperthermic and normothermic hypothalamus tissues: scores plot (PC-1 vs. PC-2) and loading corresponding to PC-2); (C) PCA results for spectra from fatal hypothermic and hyperthermic hypothalamus tissues: scores plot (PC-1 vs. PC-2) and loading corresponding to PC-2).

This is understandable because the pathophysiology processes of the hypothalamus response to fatal hypothermia and hyperthermia are different. PCA for all the three examined animal groups has been performed (Fig. S2). Fig. S2 indicates that there is a separation trend between these three groups.

Random forest feature importance analysis

It has been reported that the random forest classifier with its associated Gini feature importance allows for an explicit feature selection [70]. In this study, we performed RF to discriminate the spectral profiles of the fatal hypothermia, fatal hyperthermia and normothermia groups and further analyze the Mean Decrease Gini coefficient, one important outcome of the RF classification model, to ascertain specific spectral features that are important to the classification. Figure 4 shows the Mean Decrease in Gini Coefficient for all wavenumbers in a range. The higher the score, the more

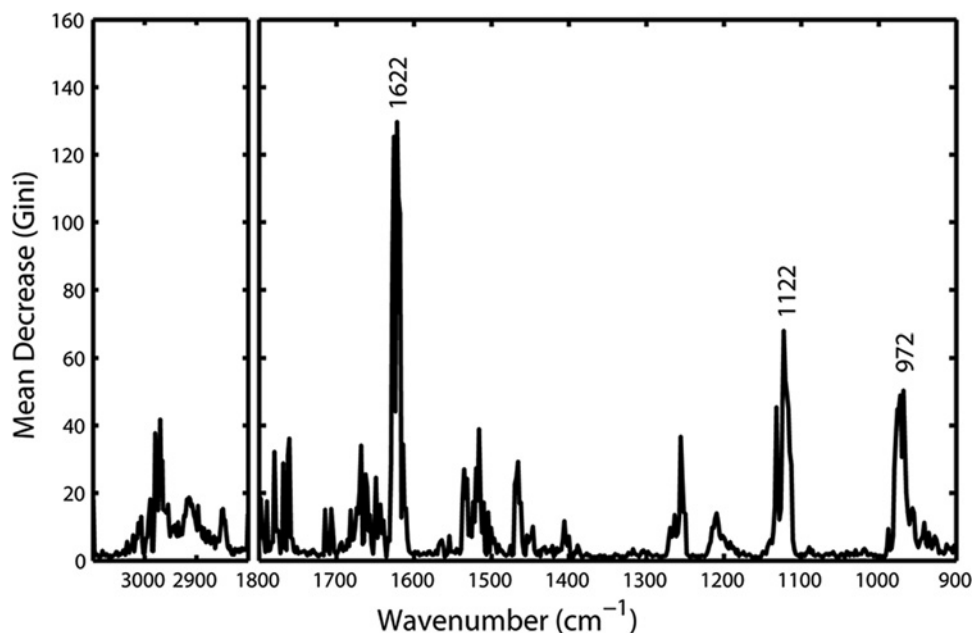


Figure 4. Gini importance chart showing the Mean Decrease in Gini coefficient for all wavenumbers in a range

important the wavenumber is to the fatal hypothermia-fatal hyperthermia-normothermia classification model. As can be seen, the prominent wavenumbers in terms of RF importance are around 1622 cm^{-1} (β -sheet secondary structures of proteins) [65], 1122 cm^{-1} (C-O stretching of ribose vibration of RNA) [71] and 972 cm^{-1} (the DNA), suggesting the major differences in spectra seen in proteins and nucleic acids are responsible for the greatest discrimination between fatal hypothermia, fatal hyperthermia and normothermia groups.

The comparison of the biochemical features among the fatal hypothermic, fatal hyperthermic and normothermic hypothalamus tissues

In this study, we successfully employed three progressive analytical methods, from the basic difference spectra analysis to unsupervised PCA, then to supervised RF machine learning method, to uncover the differences in the spectral profiles of fatal hypothermic, fatal hyperthermic and normothermic hypothalamus tissues. It was found that spectral bands around 2920 and 2850 (lipid feature), 1668, 1626, 1622 and 1518 (protein feature), 1126 (carbohydrate feature) and 1122 and 972 cm^{-1} (nucleic acids feature) were of great value for this discrimination. These findings suggested variations in the mechanisms of lipids, proteins, carbohydrates and nucleic acids across these three groups. To ascertain these mechanism differences and gain further insight into the pathophysiological processes of the hypothalamus response to fatal hypothermia and hyperthermia, these spectral features are discussed more in detail below.

Lipid region

Brain tissue contains the second highest lipid content after adipose tissue and pathological processes could result in alterations both in the content and composition of the brain lipids [72]. Figure 5 presents calculated integral intensities of selected bands and their ratios to illustrate spectral changes of lipids observed in hypothalamus. The sum of the CH_2 asymmetric and symmetric stretching modes was calculated as the content of total lipids [65] (Figure 5A). This showed the total lipid content to be significantly higher in the fatal hypothermia and hyperthermia groups when compared with normothermia group. It is thought that this is caused by the cerebral ischemia, which often occurs in deaths related to fatal hypothermia and hyperthermia, resulting in an increased production of free fatty acids [73]. The intensity of the olefinic band at 3012 cm^{-1} was used as an index of relative concentration of double bonds in the lipid structure of unsaturated lipids [74,75]. In order to examine the unsaturation level of the hypothalamus tissues, olefinic C-H/ total lipid ratio was calculated. Decreases in the olefinic C-H/ total lipid ratio both in the fatal hypothermia and hyperthermia groups with respect to the normothermia group (Figure 5B) demonstrate decreases in the concentration of unsaturated fatty acids in these two groups. These results could be attributed to lipid peroxidation, which causes the loss of olefinic bonds by breaking double bond sites of polyunsaturated acyl chains

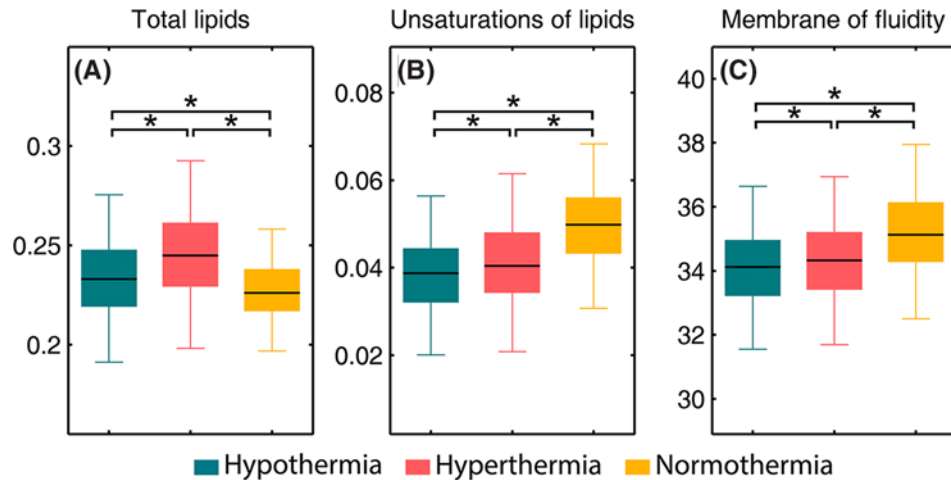


Figure 5. Selected biomarkers found in FTIR spectra

(A) total lipids ($I_{2850} + I_{2920}$), (B) unsaturation of lipids ($I_{3012} / (I_{2850} + I_{2920})$), (C) membrane fluidity (the bandwidth values of CH_2 asymmetric stretching band near 2920 cm^{-1}). An asterisk means that there is a significant difference ($P < 0.05$).

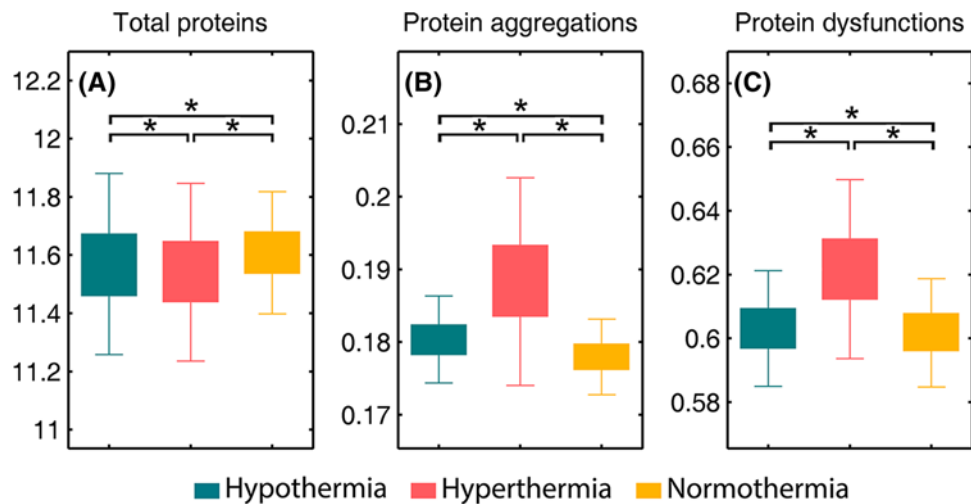


Figure 6. Selected biomarkers found in FTIR spectra

(A) total proteins ($\Sigma(I_{1600} - I_{1700})$), (B) protein aggregates (I_{1622}), (C) protein dysfunction (I_{1545} / I_{1655}). An asterisk means that there is a significant difference ($P < 0.05$).

[74]. The production of free radicals induced by cell injury is known as an important pathogenesis for lipid peroxidation [76]. Therefore, we speculate that the neurocyte injuries of hypothalamus tissues induced by fatal hypothermia and hyperthermia could produce free radicals and further result in lipid peroxidation. Additionally, the bandwidths of CH_2 asymmetric stretching bands were also measured for half of the peaks in this study. According to previous literature, these bandwidths are related to the motional rates of the molecule and are evidence of the membrane dynamics [77,78]. Significant decreases were observed in the bandwidth values of CH_2 asymmetric stretching bands of fatal hypothermia and hyperthermia groups when compared with the control group (Figure 5C), indicative of lower membrane fluidity of neurons in fatal hypothermic and hyperthermic hypothalamus tissues.

Protein region

The FTIR-based amide profiles have proven to be valuable for examining the content, structure and function of tissue proteins [67,79]. Here, the sum of intensities of protein amide I band ($1700 - 1600 \text{ cm}^{-1}$), which corresponds mainly to the $\text{C} = \text{O}$ stretching modes of the protein backbone [80], were calculated to illustrate the total protein level (Figure 6A), while the intensity of 1622 cm^{-1} was calculated to represent the level of aggregated proteins (Figure 6B) [52,53].

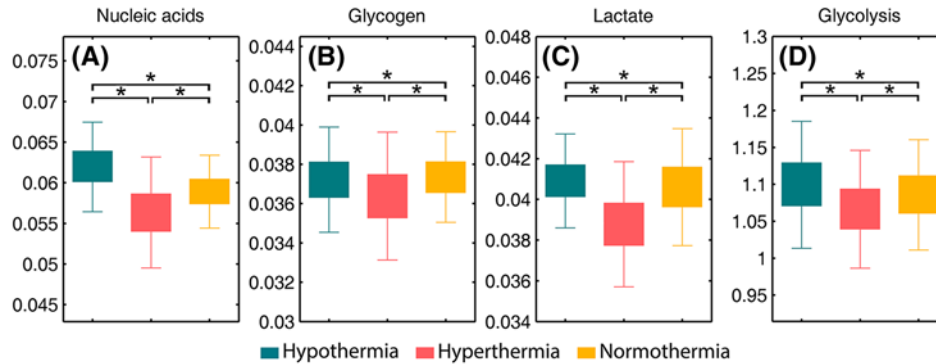


Figure 7. Selected biomarkers found in FTIR spectra

(A) total nucleic acids ($I_{1122} + I_{972}$), (B) glycogen (I_{1151}), (C) lactate (I_{1126}), (D) glycolysis (I_{1126} / I_{1151}). An asterisk means that there is a significant difference ($P < 0.05$).

Interestingly, it is observed that the fatal hyperthermia group harbors both the lowest content of total proteins and the highest content of protein aggregates among these three groups. The decreased level of total proteins could be caused by a down-regulation of proteins in the neurocyte response to heat stress [81], and the increased level of protein aggregates could be attributed to brain ischemia, which causes energy deprivation, free radical generation and antioxidant depletion as well as an increase of tissue oxidation products like protein aggregates [53]. In this study, we also calculated the ratio of amide II (maximum peak at 1545 cm^{-1}) to amide I (maximum peak at 1655 cm^{-1}), a well-known spectral marker of protein secondary structure alteration induced by various stressors [67,82,83], to represent the level of dysfunctional proteins. The graph in Figure 6C shows the highest value of the amide II/amide I ratio occurring in the fatal hyperthermia group, indicative of the most severe protein dysfunction level in fatal hyperthermic hypothalamus tissues. The three graphs in Figure 6 together demonstrate that the content, structure and function of proteins, and the cellular activity of hypothalamus tissues, are more susceptible to hyperthermia than hypothermia. Indeed, some authors point out that despite the damaging effects of hypothermia, body cooling can substantially increase the ischemic tolerance of the internal organs [84]. Our experimental data revealed a longer average death time for rats in the fatal hypothermia group than in the fatal hyperthermia group, which indirectly supports that hypothesis.

Carbohydrate and nucleic acid region

The sum of intensity at 1122 cm^{-1} (arising from RNA) and 972 cm^{-1} (arising from DNA) illustrating the total nucleic acid levels was calculated (Figure 7A). As can be observed, the total nucleic acid content is significantly lower in the fatal hyperthermia group compared with normothermia group, which is thought to be a result of heat stress. At a cellular level, this stress induces inhibition of DNA synthesis and transcription, RNA splicing and translation and cell-cycle inhibition [85,86]. A small but significant increase in the nucleic acid content for the fatal hypothermia group with respect to normothermia group is also found. This finding is in accordance with previous literature, which reported that mild hypothermia may enhance the expression of neuroprotective or repair genes to protect nervous tissues [87].

FTIR has also proved valuable for investigating carbohydrates metabolic pathways in the brain [51]. In this study, we performed absorption integration from the most specific IR bands of glycogen (1151 cm^{-1}) [51] (Figure 7B) and its one metabolic product, lactate (1126 cm^{-1}) (Figure 7C). The ratio of lactate to glycogen ($1126\text{ cm}^{-1}/1151\text{ cm}^{-1}$) was also calculated to evaluate glycolysis progress (Figure 7D). We observed that the fatal hyperthermia group contained a lower content in both glycogen and lactate in comparison with the normothermia group. This is understandable as the raised body temperature during the early pathological process of hyperthermia increases the metabolic rate and oxygen consumption, resulting in the consumption of carbohydrates [88]. Additionally, Figure 7D shows that the fatal hypothermia group has a more active glycolysis process than the hyperthermia group. It is reported that a prolonged ischemic condition could lead to the survival of cells (i.e. glia and macrophages) only capable of glycolysis metabolism [51]. Taken together, our experimental results reveal a longer average death time for rats in the fatal hypothermic tissue group than those of the fatal hyperthermic group. Previous literature has reported that heat stress not only directly affects the central nervous system and induces cytotoxicity, which kills cells, but also indirectly induces blood redistribution toward skin and muscles, resulting in neuronal necrosis [81,88]. We speculate that the

fatal hypothermia group underwent a longer period of ischemia than the fatal hyperthermia group, which led to the more active glycolysis seen in the fatal hypothermia group.

Conclusion

In this preliminary study, we demonstrate for the first time the potential of FTIR spectroscopy combined with advanced chemometrics as a method for easy and rapid assessment of the biomolecular variations seen in fatal hypothermic, fatal hyperthermic and normothermic hypothalamus tissues in rat models. Our FTIR-based results showed that the fatal hypothermic and hyperthermic hypothalamus tissues both have higher total lipid levels and lower lipid unsaturation levels, and their cell membranes demonstrated less motional freedom in comparison with the normothermic hypothalamus tissue. Additionally, the lowest total protein and carbohydrate levels and the highest protein aggregates and dysfunctions levels were observed in the fatal hyperthermic hypothalamus tissues, while the highest nucleic acid and glycolysis levels were observed in the hypothermic hypothalamus tissues.

The brain often remains unexamined in fatal hypothermia/hyperthermia death investigations because it is thought to only indicate nonspecific histopathological findings. Nevertheless, our FTIR-based results show that the biochemical profiles of fatal hypothermic, fatal hyperthermic and normothermic hypothalamus tissues were significantly different. This study, supported by our previous studies [89,90], demonstrates that some tissues or organs regarded as nonspecific for the determination of the cause of death in forensic pathology do indeed have specific biochemical fingerprints. There is a high potential for this technique to augment the results of conventional forensic post-mortem examination and provide for a more accurate determination of the cause of death. Nevertheless, much work still needs to be done both by our own group and by others. It is important to acknowledge that we need to investigate the biochemical signatures of hypothalamus tissues from alternative causes of death, such as fatal anaphylactic shock, drowning, sudden cardiac death, neurological failures and intoxication-related deaths. These are common causes of death encountered in forensic casework and should be taken into consideration in the control groups of further studies like this one.

Funding

This project was supported by grants from the National Key R&D Program of China [2016YFC0800702]; the National Natural Science Foundation of China [81730056, 81722027, 81801873, 81601645 and 81671869]; and the Science and Technology Committee of Shanghai Municipality [17DZ2273200 and 16DZ2290900].

Competing Interests

The authors declare that there are no competing interests associated with the manuscript.

Author Contribution

Ping Huang, Zhenyuan Wang and Hancheng Lin designed this research project. Kaifei Deng, Ji Zhang, Lei Wang and Zhong Zhang performed the experiments. Hancheng Lin, Kaifei Deng, Yiwen Luo, Qiran Sun and Zhengdong Li analyzed the results. Hancheng Lin and Kaifei Deng wrote this manuscript. Yijiu Chen prepared the figures. All authors reviewed the manuscript.

Abbreviations

EMSC, extended multiplicative signal correction; FTIR, fourier-transform infrared; H&E, hematoxylin & eosin; PCA, principle component analysis; RF, random forest.

References

- Charkoudian, N. (2003) Skin blood flow in adult human thermoregulation: how it works, when it does not, and why. *Mayo Clin. Proc.* **78**, 603, <https://doi.org/10.4065/78.5.603>
- Palmiere, C. and Mangin, P. (2013) Hypothalamus tissues of fatal hypothermic, fatal hyperthermic and normothermic rats. *Int. J. Legal Med.* **127**, 93, <https://doi.org/10.1007/s00414-012-0722-6>
- Palmiere, C., Teresiński, G. and Hejna, P. (2014) Postmortem diagnosis of hypothermia. *Int. J. Legal Med.* **128**, 607, <https://doi.org/10.1007/s00414-014-0977-1>
- Palmiere, C. and Mangin, P. (2013) Postmortem biochemical investigations in hypothermia fatalities. *Int. J. Legal Med.* **127**, 267, <https://doi.org/10.1007/s00414-012-0738-y>
- Turk, E.E. (2010) Hypothermia. *Forensic Sci. Med. Pathol.* **6**, 106, <https://doi.org/10.1007/s12024-010-9142-4>
- Seidl, S. (2009) Tsokos, M. (ed.): Forensic Pathology Reviews, Vol 5. *Forensic Sci. Med. Pathol.* **5**, 246, <https://doi.org/10.1007/s12024-009-9073-0>
- Doberentz, E. and Madea, B. (2017) Microscopic examination of pituitary glands in cases of fatal accidental hypothermia. *Forensic Sci. Res.* **2**, 132, <https://doi.org/10.1080/20961790.2017.1330804>

- 8 Bańka, K., Teresiński, G. and Buszewicz, G. (2014) Free fatty acids as markers of death from hypothermia. *Forensic Sci. Int.* **234**, 79, <https://doi.org/10.1016/j.forsciint.2013.10.028>
- 9 Pakanen, L., Kaija, H., Kortelainen, M.L., Särkioja, T. and Porvari, K. (2015) Victims of lethal hypothermia have decreased levels of thrombomodulin in myocardium and urine. *Int. J. Legal Med.* **129**, 289, <https://doi.org/10.1007/s00414-014-1138-2>
- 10 Yajima, D., Asari, M., Okuda, K., Maseda, C., Yamada, H., Ichimaru, C. et al. (2015) An objective approach using three indexes for determining fatal hypothermia due to cold exposure; statistical analysis of oxyhemoglobin saturation data. *Leg. Med.* **17**, 451, <https://doi.org/10.1016/j.legalmed.2015.09.005>
- 11 Palmiere, C., Bardy, D., Letovanec, I., Mangin, P., Augsburger, M., Ventura, F. et al. (2013) Biochemical markers of fatal hypothermia. *Forensic Sci. Int.* **226**, 54, <https://doi.org/10.1016/j.forsciint.2012.12.007>
- 12 Bańka, K., Teresiński, G., Buszewicz, G. and Mađro, R. (2013) Glucocorticosteroids as markers of death from hypothermia. *Forensic Sci. Int.* **229**, 60, <https://doi.org/10.1016/j.forsciint.2013.03.003>
- 13 Kaija, H., Pakanen, L., Uusitalo, J., Nikkilä, S., Kortelainen, M.L. and Porvari, K.S. (2014) Changes in cardiac thrombomodulin and heat shock transcription factor 1 expression and peripheral thrombomodulin and catecholamines during hypothermia in rats. *Stress* **17**, 504, <https://doi.org/10.3109/10253890.2014.953477>
- 14 Descloux, E., Augsburger, M., Teresiński, G., Hejna, P., Grouzmann, E., Scarpelli, M.P. et al. (2017) Endocan concentrations in postmortem serum, vitreous humor and urine in victims of lethal hypothermia. *J. Forensic Legal Med.* **50**, 39, <https://doi.org/10.1016/j.jflm.2017.07.002>
- 15 Doberentz, E., Markwerth, P., Wagner, R. and Madea, B. (2017) Expression of Hsp27 and Hsp70 and vacuolization in the pituitary glands in cases of fatal hypothermia. *Forensic Sci. Med. Pathol.* **13**, 312, <https://doi.org/10.1007/s12024-017-9884-3>
- 16 Hervet, T., Teresiński, G., Hejna, P., Descloux, E., Grouzmann, E. and Palmiere, C. (2016) Catecholamines and their O -methylated metabolites in vitreous humor in hypothermia cases. *Forensic Sci. Med. Pathol.* **12**, 163, <https://doi.org/10.1007/s12024-016-9764-2>
- 17 Song, K., Wang, H., Kamm, G.B., Pohle, J., Reis, F.C., Heppenstall, P. et al. (2016) The TRPM2 channel is a hypothalamic heat sensor that limits fever and can drive hypothermia.. *Science* **353**, 1393, <https://doi.org/10.1126/science.aaf7537>
- 18 Ishikawa, T., Yoshida, C. and Michiue, T. (2010) Immunohistochemistry of catecholamines in the hypothalamic–pituitary–adrenal system with special regard to fatal hypothermia and hyperthermia. *Leg. Med.* **12**, 121, <https://doi.org/10.1016/j.legalmed.2010.01.004>
- 19 Yoshida, C., Ishikawa, T., Michiue, T., Quan, L. and Maeda, H. (2011) Postmortem biochemistry and immunohistochemistry of chromogranin A as a stress marker with special regard to fatal hypothermia and hyperthermia. *Int. J. Legal Med.* **125**, 11, <https://doi.org/10.1007/s00414-009-0374-3>
- 20 Prati, S., Joseph, E., Sciutto, G. and Mazzeo, R. (2010) New advances in the application of FTIR microscopy and spectroscopy for the characterization of artistic materials. *Acc. Chem. Res.* **43**, 792, <https://doi.org/10.1021/ar900274f>
- 21 Wrobel, T.P. and Bhargava, R. (2017) Infrared spectroscopic imaging advances as an analytical technology for biomedical sciences. *Anal. Chem.* **90**, 1444, <https://doi.org/10.1021/acs.analchem.7b05330>
- 22 Petitbois, C. and Desbat, B. (2010) Clinical application of FTIR imaging: new reasons for hope. *Trends Biotechnol.* **28**, 495, <https://doi.org/10.1016/j.tibtech.2010.07.003>
- 23 Baker, M.J., Hussain, S.R., Lovergne, L., Untereiner, V., Hughes, C., Lukaszewski, R.A. et al. (2015) Developing and understanding biofluid vibrational spectroscopy: a critical review. *Chem. Soc. Rev.* **45**, 1803, <https://doi.org/10.1039/C5CS00585J>
- 24 Bird, B. and Rowlette, J. (2017) High definition infrared chemical imaging of colorectal tissue using a Spero QCL microscope. *Analyst* **142**, 1381, <https://doi.org/10.1039/C6AN01916A>
- 25 Bao, W., Li, J., Li, J., Zhang, Q., Liu, Y., Shi, C. et al. (2018) Au/ZnSe-Based Surface Enhanced Infrared Absorption Spectroscopy as a Universal Platform for Bioanalysis. *Anal. Chem.* **90**, 3842, <https://doi.org/10.1021/acs.analchem.7b04505>
- 26 Perez-Guaita, D., Kochan, K., Batty, M., Doerig, C., Garcia-Bustos, J., Espinoza, S. et al. (2018) Multispectral atomic force microscopy-infrared nano-imaging of malaria infected red blood cells. *Anal. Chem.* **90**, 3140, <https://doi.org/10.1021/acs.analchem.7b04318>
- 27 Byrne, H.J., Knief, P., Keating, M.E. and Bonnier, F. (2016) Spectral pre and post processing for infrared and Raman spectroscopy of biological tissues and cells.. *Chem. Soc. Rev.* **45**, 1865
- 28 Baker, M.J., Trevisan, J., Bassan, P., Bhargava, R., Butler, H.J., Dorling, K.M. et al. (2014) Using Fourier transform IR spectroscopy to analyze biological materials. *Nat. Protoc.* **9**, 1771, <https://doi.org/10.1038/nprot.2014.110>
- 29 Kendall, C., Isabelle, M., Bazant-Hegemark, F., Hutchings, J., Orr, L., Babrah, J. et al. (2009) Vibrational spectroscopy: a clinical tool for cancer diagnostics. *Analyst* **134**, 1029, <https://doi.org/10.1039/b822130h>
- 30 Ly, E., Piot, O., Durlach, A., Bernard, P. and Manfait, M. (2009) Differential diagnosis of cutaneous carcinomas by infrared spectral micro-imaging combined with pattern recognition. *Analyst* **134**, 1208, <https://doi.org/10.1039/b820998g>
- 31 Verdonck, M., Denayer, A., Delvaux, B., Garaud, S., De, W.R., Desmedt, C. et al. (2016) Characterization of human breast cancer tissues by infrared imaging. *Analyst* **141**, 606, <https://doi.org/10.1039/C5AN01512J>
- 32 Chrabaszcz, K., Kochan, K., Fedorowicz, A., Jaształ, A., Buczek, E., Leslie, L.S. et al. (2018) FT-IR- and Raman-based biochemical profiling of the early stage of pulmonary metastasis of breast cancer in mice. *Analyst*, <https://doi.org/10.1039/C7AN01883E>
- 33 Walsh, M.J., Singh, M.N., Stringfellow, H.F., Pollock, H.M., Azzedine, H., Olaug, G. et al. (2008) FTIR Microspectroscopy Coupled with Two-Class Discrimination Segregates Markers Responsible for Inter- and Intra-Category Variance in Exfoliative Cervical Cytology.. *Biomark Insights* **3**, 179, <https://doi.org/10.4137/BMI.S592>
- 34 Nallala, J., Diebold, M.D., Gobinet, C., Bouchā, O., Sockalingum, G.D., Piot, O. et al. (2014) Infrared spectral histopathology for cancer diagnosis: a novel approach for automated pattern recognition of colon adenocarcinoma. *Analyst* **139**, 4005, <https://doi.org/10.1039/C3AN01022H>
- 35 Pucetaite, M., Velicka, M., Urboniene, V., Ceponkus, J., Bandzeviciute, R., Jankevicius, F. et al. (2018) Rapid intra-operative diagnosis of kidney cancer by ATR-IR spectroscopy of tissue smears.. *J. Biophotonics*

- 36 Sharaha, U., Rodriguezdiaz, E., Riesenber, K., Bigio, I.J., Huleihel, M. and Salman, A. (2017) Using Infrared Spectroscopy and Multivariate Analysis to Detect Antibiotics' Resistant *Escherichia coli* Bacteria. *Anal. Chem.* **89**, 8782, <https://doi.org/10.1021/acs.analchem.7b01025>
- 37 Rymysa, T., Ribeiro, E.A., De, L.C., Bhattacharjee, T. and De, R. A.C. (2018) Human papillomavirus detection using PCR and ATR-FTIR for cervical cancer screening. *Spectrochim. Acta, Part A* **196**, 238, <https://doi.org/10.1016/j.saa.2018.02.004>
- 38 Wood, B.R., Bamberg, K.R., Dixon, M.W., Tilley, L., Nasse, M.J., Mattson, E. et al. (2014) Diagnosing malaria infected cells at the single cell level using focal plane array Fourier transform infrared imaging spectroscopy. *Analyst* **139**, 4769, <https://doi.org/10.1039/C4AN00989D>
- 39 Bhattacharjee, T.T., Nicodemo, M.C., Sant'Anna, L.B., Arisawa, E. A. L.S. and Raniero, L. (2018) Tendinopathy diagnosis and treatment monitoring using attenuated total reflectance-Fourier transform infrared spectroscopy. *J. Biophotonics* **11**, e201700256, <https://doi.org/10.1002/jbio.201700256>
- 40 Cerusico, N., Aybar, J.P., Lopez, S., Molina, S.G., Chavez, R.J., Cabral, M. E.S. et al. (2018) FTIR spectroscopy of chronic venous leg ulcer exudates: an approach to spectral healing marker identification. *Analyst* **143**, 1583, <https://doi.org/10.1039/C7AN01909B>
- 41 Palombo, F., Tamagnini, F., Jeynes, J., Mattana, S., Swift, I., Nallala, J. et al. (2018) Detection of A β plaque-associated astrogliosis in Alzheimer's disease brain by spectroscopic imaging and immunohistochemistry. *Analyst* **143**, 850, <https://doi.org/10.1039/C7AN01747B>
- 42 Summers, K.L., Fimognari, N., Hollings, A., Kiernan, M., Lam, V., Tidy, R.J. et al. (2017) A Multimodal Spectroscopic Imaging Method To Characterize the Metal and Macromolecular Content of Proteinaceous Aggregates ("Amyloid Plaques"). *Biochemistry* **56**, 4107, <https://doi.org/10.1021/acs.biochem.7b00262>
- 43 Liao, C.R., Rak, M., Lund, J., Unger, M., Platt, E., Albensi, B.C. et al. (2013) Synchrotron FTIR reveals lipid around and within amyloid plaques in transgenic mice and Alzheimer's disease brain. *Analyst* **138**, 3991, <https://doi.org/10.1039/c3an00295k>
- 44 Leskovjan, A.C., Kretlow, A. and Miller, L.M. (2010) Fourier transform infrared imaging showing reduced unsaturated lipid content in the hippocampus of a mouse model of Alzheimer's disease. *Anal. Chem.* **82**, 2711, <https://doi.org/10.1021/ac1002728>
- 45 Araki, K., Yagi, N., Ikemoto, Y., Yagi, H., Choong, C.J., Hayakawa, H. et al. (2015) Synchrotron FTIR micro-spectroscopy for structural analysis of Lewy bodies in the brain of Parkinson's disease patients. *Sci. Rep.* **5**, 17625, <https://doi.org/10.1038/srep17625>
- 46 Ahmed, S. S. S.J., Santosh, W., Kumar, S. and Christlet, T. H.T. (2010) Neural network algorithm for the early detection of Parkinson's disease from blood plasma by FTIR micro-spectroscopy. *Vib. Spectrosc.* **53**, 181, <https://doi.org/10.1016/j.vibspec.2010.01.019>
- 47 Szczerbawska-Boruchowska, M., Dumas, P., Kastyak, M., Chwiej, J., Lankosz, M., Adamek, D. et al. (2007) Biomolecular investigation of human substantia nigra in Parkinson's disease by synchrotron radiation Fourier transform infrared micro spectroscopy. *Arch. Biochem. Biophys.* **459**, 241, <https://doi.org/10.1016/j.abb.2006.12.027>
- 48 Heraud, P., Caine, S., Campanale, N., Karnezis, T., Mcnaughton, D., Wood, B.R. et al. (2010) Early detection of the chemical changes occurring during the induction and prevention of autoimmune-mediated demyelination detected by FT-IR imaging. *NeuroImage* **49**, 1180, <https://doi.org/10.1016/j.neuroimage.2009.09.053>
- 49 Miller, L.M., Bourassa, M.W. and Smith, R.J. (2013) FTIR spectroscopic imaging of protein aggregation in living cells. *Biochim. Biophys. Acta* **1828**, 2339, <https://doi.org/10.1016/j.bbamem.2013.01.014>
- 50 Hackett, M.J., Aitken, J.B., El-Assaad, F., Mcquillan, J.A., Carter, E.A., Ball, H.J. et al. (2015) Mechanisms of murine cerebral malaria: Multimodal imaging of altered cerebral metabolism and protein oxidation at hemorrhage sites. *Sci. Adv.* **1**, e1500911, <https://doi.org/10.1126/sciadv.1500911>
- 51 Hackett, M.J., Sylvain, N.J., Hou, H., Caine, S., Alavardashvili, M., Pushie, M.J. et al. (2016) Concurrent Glycogen and Lactate Imaging with FTIR Spectroscopy to Spatially Localize Metabolic Parameters of the Glial Response following Brain Ischemia. *Anal. Chem.* **88**, 10949, <https://doi.org/10.1021/acs.analchem.6b02588>
- 52 Caine, S., Hackett, M.J., Hou, H., Kumar, S., Maley, J., Ivanishvili, Z. et al. (2016) A novel multi-modal platform to image molecular and elemental alterations in ischemic stroke. *Neurobiol. Dis.* **91**, 132, <https://doi.org/10.1016/j.nbd.2016.03.006>
- 53 Hackett, M.J., Britz, C.J., Paterson, P.G., Nichol, H., Pickering, I.J. and George, G.N. (2015) In Situ Biospectroscopic Investigation of Rapid Ischemic and Postmortem Induced Biochemical Alterations in the Rat Brain. *ACS Chem. Neurosci.* **6**, 226, <https://doi.org/10.1021/cn500157j>
- 54 Hackett, M.J., Smith, S.E., Caine, S., Nichol, H., George, G.N., Pickering, I.J. et al. (2015) Novel bio-spectroscopic imaging reveals disturbed protein homeostasis and thiol redox with protein aggregation prior to hippocampal CA1 pyramidal neuron death induced by global brain ischemia in the rat. *Free Radical Biol. Med.* **89**, 806, <https://doi.org/10.1016/j.freeradbiomed.2015.08.029>
- 55 Hackett, M.J., Desouza, M., Caine, S., Bewer, B., Nichol, H., Paterson, P.G. et al. (2015) A new method to image heme-fe, total fe, and aggregated protein levels after intracerebral hemorrhage. *ACS Chem. Neurosci.* **6**, 761, <https://doi.org/10.1021/acschemneuro.5b00037>
- 56 Turker, S., Severcan, M., Ilbay, G. and Severcan, F. (2014) Epileptic seizures induce structural and functional alterations on brain tissue membranes. *Biochim. Biophys. Acta* **1838**, 3088, <https://doi.org/10.1016/j.bbamem.2014.08.025>
- 57 Garip, S., Sahin, D. and Severcan, F. (2013) Epileptic seizure-induced structural and functional changes in rat femur and tibia bone tissues: a Fourier transform infrared imaging study. *J. Biomed. Opt.* **18**, 111409, <https://doi.org/10.1117/1.JBO.18.11.111409>
- 58 Seeley, R., VanPutte, C., Regan, J. and Russo, A. (2014) *Seeley's Anatomy & Physiology*, 10th edn, McGraw-Hill Companies, Inc., New York
- 59 Zhou, C., Bright, F., Winskog, C., Yool, A.J. and Byard, R.W. (2014) Lethal hypothermia in an animal model, not associated with basal renal epithelial vacuolization. *J. Forensic & Legal Med.* **21**, 14, <https://doi.org/10.1016/j.jflm.2013.10.014>
- 60 Wang, Z., Tuo, Y., Bing, L., Deng, K., Han, S., Luo, Y. et al. (2017) Preliminary study on fatal hyperthermia in rat liver tissue by Fourier transform infrared microspectroscopy. *Aust. J. Forensic Sci.* **49**, 468, <https://doi.org/10.1080/00450618.2016.1156157>
- 61 Afseth, N.K. and Kohler, A. (2012) Extended multiplicative signal correction in vibrational spectroscopy, a tutorial. *Chemometrics Intell. Lab. Syst.* **117**, 92, <https://doi.org/10.1016/j.chemolab.2012.03.004>
- 62 Smilde, A.K. and Bro, R. (2014) Principal component analysis. *Anal. Methods* **6**, 2812, <https://doi.org/10.1039/C3AY41907J>
- 63 Smith, B.R., Ashton, K.M., Brodbelt, A., Dawson, T., Jenkinson, M.D., Hunt, N.T. et al. (2016) Combining random forest and 2D correlation analysis to identify serum spectral signatures for neuro-oncology. *Analyst* **141**, 3668, <https://doi.org/10.1039/C5AN02452H>
- 64 Dettmeyer, R.B. (2011) *Forensic Histopathology: Fundamentals and Perspectives*, 1st edn, Springer Science & Business Media, New York

- 65 Caine, S., Heraud, P., Tobin, M.J., Mcnaughton, D. and Bernard, C. C.A. (2012) The application of Fourier transform infrared microspectroscopy for the study of diseased central nervous system tissue. *NeuroImage* **59**, 3624, <https://doi.org/10.1016/j.neuroimage.2011.11.033>
- 66 Petibois, C., Goupillou, G., Wehbe, K., Delage, J.P. and Dél  ris, G. (2006) Analysis of type I and IV collagens by FT-IR spectroscopy and imaging for a molecular investigation of skeletal muscle connective tissue. *Anal. Bioanal. Chem.* **386**, 1961, <https://doi.org/10.1007/s00216-006-0828-0>
- 67 Staniszewska-Slezak, E., Wiercigroch, E., Fedorowicz, A., Buczek, E., Mateuszuk, L., Baranska, M. et al. (2018) A possible Fourier transform infrared-based plasma fingerprint of angiotensin-converting enzyme inhibitor-induced reversal of endothelial dysfunction in diabetic mice. *J. Biophotonics* **11**, e201700044, <https://doi.org/10.1002/jbio.201700044>
- 68 Uckermann, O., Juratli, T.A., Galli, R., Conde, M., Wiedemuth, R., Krex, D. et al. (2017) Optical analysis of glioma: Fourier-transform infrared spectroscopy reveals the IDH1 mutation status. *Clin. Cancer Res.* **17**, 1795
- 69 Morato, E.M., Morais, G.R., Sato, F., Medina, A.N., Svidzinski, T.I., Baesso, M.L. et al. (2013) Morphological and structural changes in lung tissue infected by paracoccidioides brasiliensis : FTIR photoacoustic spectroscopy and histological analysis. *Photochem. Photobiol.* **89**, 1170, <https://doi.org/10.1111/php.12110>
- 70 Menze, B.H., Kelm, B.M., Masuch, R., Himmelreich, U., Bachert, P., Petrich, W. et al. (2009) A comparison of random forest and its Gini importance with standard chemometric methods for the feature selection and classification of spectral data. *BMC Bioinf.* **10**, 1, <https://doi.org/10.1186/1471-2105-10-213>
- 71 Sahu, R.K., Argov, S., Salman, A., Huleihel, M., Grossman, N., Hammody, Z. et al. (2004) Characteristic absorbance of nucleic acids in the Mid-IR region as possible common biomarkers for diagnosis of malignancy. *Technol. Cancer Res. Treat.* **3**, 629, <https://doi.org/10.1177/153303460400300613>
- 72 Yonar, D., Ocek, L., Tiftikcioglu, B.I., Zorlu, Y. and Severcan, F. (2018) Relapsing-Remitting Multiple Sclerosis diagnosis from cerebrospinal fluids via Fourier transform infrared spectroscopy coupled with multivariate analysis. *Sci. Rep.* **8**, 1025, <https://doi.org/10.1038/s41598-018-19303-3>
- 73 Yoshida, S., Inoh, S., Asano, T., Sano, K., Kubota, M., Shimazaki, H. et al. (1980) Effect of transient ischemia on free fatty acids and phospholipids in the gerbil brain. Lipid peroxidation as a possible cause of postischemic injury. *J. Neurosurg.* **53**, 323, <https://doi.org/10.3171/jns.1980.53.3.0323>
- 74 Cakmak, G., Miller, L.M., Zorlu, F. and Severcan, F. (2012) Amifostine, a radioprotectant agent, protects rat brain tissue lipids against ionizing radiation induced damage: an FTIR microspectroscopic imaging study. *Arch. Biochem. Biophys.* **520**, 67, <https://doi.org/10.1016/j.abb.2012.02.012>
- 75 Stitt, D.M., Kastyak-Ibrahim, M.Z., Liao, C.R., Morrison, J., Albensi, B.C. and Gough, K.M. (2012) Tissue acquisition and storage associated oxidation considerations for FTIR microspectroscopic imaging of polyunsaturated fatty acids. *Vib. Spectrosc.* **60**, 16, <https://doi.org/10.1016/j.vibspec.2011.10.016>
- 76 Gutteridge, J.M. (1995) Lipid peroxidation and antioxidants as biomarkers of tissue damage. *Clin. Chem.* **41**, 1819
- 77 Yonar, D. and Sunnetcioglu, M.M. (2016) Effect of cis-(Z)-flupentixol on DPPC membranes in the presence and absence of cholesterol. *Chem. Phys. Lipids* **198**, 61, <https://doi.org/10.1016/j.chemphyslip.2016.06.002>
- 78 Severcan, F., Sahin, I. and Kazanc, N. (2005) Melatonin strongly interacts with zwitterionic model membranes—evidence from Fourier transform infrared spectroscopy and differential scanning calorimetry. *Biochim. Biophys. Acta* **1668**, 215, <https://doi.org/10.1016/j.bbamem.2004.12.009>
- 79 G  ler, G., Acikgoz, E., Karabay, N.Y., Bakan, B., Goormaghtigh, E. and Aktug, H. (2018) Deciphering the biochemical similarities and differences among mouse embryonic stem cells, somatic and cancer cells using ATR-FTIR spectroscopy. *Analyst* **143**, 1624, <https://doi.org/10.1039/C8AN00017D>
- 80 Yang, H., Yang, S., Kong, J., Dong, A. and Yu, S. (2015) Obtaining information about protein secondary structures in aqueous solution using Fourier transform IR spectroscopy. *Nat. Protoc.* **10**, 382, <https://doi.org/10.1038/nprot.2015.024>
- 81 Dewhirst, M.W., Vigilanti, B.L., Loramichiels, M., Hanson, M. and Hoopes, P.J. (2003) Basic principles of thermal dosimetry and thermal thresholds for tissue damage from hyperthermia. *Int. J. Hyperthermia* **19**, 267, <https://doi.org/10.1080/0265673031000119006>
- 82 Bramanti, E., Lenci, F. and Sgarbossa, A. (2010) Effects of hypericin on the structure and aggregation properties of β -amyloid peptides. *Eur. Biophys. J.* **39**, 1493, <https://doi.org/10.1007/s00249-010-0607-x>
- 83 Litvinov, R., Faizullin, D., Zuev, Y. and Weisel, J. (2012) The α -Helix to β -Sheet Transition in Stretched and Compressed Hydrated Fibrin Clots. *Biophys. J.* **103**, 1020, <https://doi.org/10.1016/j.bpj.2012.07.046>
- 84 Jennett, B. (1997) Treatment of Traumatic Brain Injury with Moderate Hypothermia. *N. Engl. J. Med.* **336**, 540, <https://doi.org/10.1056/NEJM199702203360803>
- 85 Yan, Y.E., Zhao, Y.Q., Wang, H. and Fan, M. (2006) Pathophysiological factors underlying heatstroke. *Med. Hypotheses* **67**, 609, <https://doi.org/10.1016/j.mehy.2005.12.048>
- 86 Sonna, L.A., Fujita, J., Gaffin, S.L. and Lilly, C.M. (2002) Invited review: Effects of heat and cold stress on mammalian gene expression. *J. Appl. Physiol.* **92**, 1725, <https://doi.org/10.1152/jappphysiol.01143.2001>
- 87 Dietrich, W.D., Therapeutic hypothermia in experimental models of traumatic brain injury In: Hayashi, N. (ed) (2000) *Brain Hypothermia: Pathology, Pharmacology, and Treatment of Severe Brain Injury*, pp. 39–46, Springer Science & Business Media, New York
- 88 Ceausu, M., Hostiuc, S., Dan, D. and Curca, G.C. (2010) Morphological diagnosis of hyperthermia-related deaths. *Romanian J. Legal Med.* **18**, 239, <https://doi.org/10.4323/rjlm.2010.239>
- 89 Lin, H., Luo, Y., Wang, L., Deng, K., Sun, Q., Fang, R. et al. (2018) Identification of pulmonary edema in forensic autopsy cases of fatal anaphylactic shock using Fourier transform infrared microspectroscopy. *Int. J. Legal Med.* **132**, 477, <https://doi.org/10.1007/s00414-017-1721-4>
- 90 Lin, H., Luo, Y., Sun, Q., Zhang, J., Tuo, Y., Zhang, Z. et al. (2018) Identification of pulmonary edema in forensic autopsy cases of sudden cardiac death using Fourier transform infrared microspectroscopy: a pilot study. *Anal. Chem.* **90**, 2708, <https://doi.org/10.1021/acs.analchem.7b04642>